Fluorescence correlation spectroscopy experiments to quantify free diffusion coefficients in reaction-diffusion systems: The case of Ca^{2+} and its dyes

Lorena Sigaut, Cecilia Villarruel,* María Laura Ponce, and Silvina Ponce Dawson
Departamento de Física, FCEN-UBA, and IFIBA, CONICET, Ciudad Universitaria, Pabellón I, (1428) Buenos Aires, Argentina
(Received 1 August 2016; revised manuscript received 3 March 2017; published 12 June 2017)

Many cell signaling pathways involve the diffusion of *messengers* that bind and unbind to and from intracellular components. Quantifying their net transport rate under different conditions then requires having separate estimates of their free diffusion coefficient and binding or unbinding rates. In this paper, we show how performing sets of *fluorescence correlation spectroscopy* (FCS) experiments under different conditions, it is possible to quantify free diffusion coefficients and on and off rates of reaction-diffusion systems. We develop the theory and present a practical implementation for the case of the universal second messenger, calcium (Ca^{2+}) and single-wavelength dyes that increase their fluorescence upon Ca^{2+} binding. We validate the approach with experiments performed in aqueous solutions containing Ca^{2+} and Fluo4 dextran (both in its high and low affinity versions). Performing FCS experiments with tetramethylrhodamine-dextran in *Xenopus laevis* oocytes, we infer the corresponding free diffusion coefficients in the cytosol of these cells. Our approach can be extended to other physiologically relevant reaction-diffusion systems to quantify biophysical parameters that determine the dynamics of various variables of interest.

DOI: 10.1103/PhysRevE.95.062408

I. INTRODUCTION

Many cell signaling pathways involve the diffusion of messengers in the cytoplasm. In most cases these substances convey their message by binding to target molecules. Furthermore, as they reach their targets they not only diffuse freely but also bind and unbind to and from other cell components. For long enough times, the net transport that results from the combination of free diffusion and binding or unbinding is described by *effective diffusion coefficients* that are weighted averages of the free coefficients of the messenger and of the substance it interacts with [1]. Differently from free coefficients, effective coefficients depend on the concentrations of the reactants and on reaction rates. The universal second messenger calcium (Ca^{2+}) provides a prototypical example of this behavior. Persistently high cytosolic Ca^{2+} concentrations lead to cell death. For this reason, cells have numerous mechanisms to reduce this concentration, the fastest one of which is *buffering*. Buffers are molecules that bind and unbind to and from Ca^{2+} ions reducing their free concentration, altering their spatiotemporal distribution [2,3] and the eventually evoked end responses [4]. The cytosolic Ca^{2+} concentration can attain very different values. The resulting Ca^{2+} effective diffusion coefficient then varies across disparate values depending on the signal type. The range of values was estimated as $\sim [5,220]\ \mu\mathbf{m}^2/s$ [5] with increasing values as the cytosolic Ca^{2+} concentration increased. How fast can Ca^{2+} diffuse inside cells? In order to answer this question it is necessary to have separate estimates of the Ca^{2+} and Ca^{2+} buffers free diffusion coefficients, their concentrations, and reactions rates. Ideally, having access to this information one could eventually compute the Ca^{2+} effective diffusion coefficient as a function of its concentration. Ca^{2+} images do not provide direct information on Ca^{2+} transport because the fluorescence that is collected comes from the dye (either free or Ca^{2+}-bound), not from the free Ca^{2+} concentration. In the case of the single-wavelength dyes [6,7] that increase their fluorescence intensity when bound to Ca^{2+}, the Ca^{2+} currents that can be inferred from the images [8] are very sensitive to uncertainties in the on rate of the Ca^{2+}-dye binding reaction and in the diffusion coefficient of the dye [9]. Having reliable estimates of these parameters is thus unavoidable to extract quantitative information from the images. In this paper, we describe and implement an approach that shows how performing sets of *fluorescence correlation spectroscopy* (FCS) [10] experiments under different conditions and using a reaction-diffusion model to interpret the experimental results it is possible to obtain separate estimates of the free Ca^{2+} and dye diffusion coefficients and of the rates of their binding and unbinding reaction.

In FCS, the fluorescence intensity in a small volume is recorded along time and, via an analysis of the temporal autocorrelation of the observed fluctuations, the transport rates of the fluorescent species are, in principle, derived [11]. FCS has been widely used to determine the diffusion coefficients of fluorescently labeled proteins inside cells [12–14]. When the fluorescent species diffuse freely in the medium there is an analytic expression for the autocorrelation function of the fluorescent fluctuations (ACF) that is used to fit the experimental observations and derive diffusion coefficients (see Materials and Methods). When the fluorescent particles diffuse and react, simple analytic expressions for the ACF can only be obtained under certain approximations [11,15–20]. Depending on the relative timescales of the problem it is also possible to quantify reaction rates using FCS [11,16,17]. In fact, the paper where the method was introduced [11] presented an application in which the reaction rates of a bimolecular reaction were derived for a situation in which the lightest reactant was in excess. A similar situation was considered in Ref. [16], in which an enhanced version of FCS was introduced to improve the signal to noise ratio. Deriving the reaction rates of a bimolecular reaction from FCS experiments was also the aim of the work in Ref. [17]. In all these examples, the concentrations of the reactants were assumed to be known *a*

*Corresponding author: cvillarruel@df.uba.ar

priori and the experiments were performed to infer kinetic parameters. The lightest reactant, on the other hand, was the marker that increased its fluorescence upon binding to the heaviest one, the latter being the biological relevant molecule. Fluctuations were then due to binding or unbinding and diffusion and by exploiting the timescale separation between both of them the reaction rates were determined [11,16,17]. In the present paper, we are also interested in a system in which diffusion and reactions occur. But, as in our previous works [18–21], the situation of interest is such that the biologically relevant species (Ca^{2+} in this paper, a fluorescent protein in the previous ones) is the lightest reactant and the quantification of its free (rather than effective) diffusion coefficient is the main purpose of the investigation. In the case of fluorescently tagged proteins, the reactions correspond to interactions with more massive (nonfluorescent) molecules that hinder their transport [21]. In the present paper, the reactions occur with (more massive) probes that allow the species of interest to be observed. As shown for the case of fluorescently labeled proteins in Refs. [18–20], when the reactions act on a somewhat faster timescale than diffusion, the correlation times of the fluctuations are associated to the free diffusion coefficient of the most massive reactant (if it is mobile) and to the effective coefficients mentioned before. As analyzed theoretically in Refs. [18,20], even though the reaction time does not characterize per se the decay of the ACF, it is still possible to quantify some of the reaction parameters via the dependence of the (effective) diffusive timescales on them. In this paper, we present a practical implementation of these ideas but for a system in which the reactions are necessary for the fluorescence to be readily observable, as in the situations probed in Refs. [11,16,17]. In such a case, one of the timescales that characterizes the decay of the ACF is determined by the reaction time. Thus, on and off rates, not just the dissociation constant as done in Ref. [21], could in principle be derived. We envisage the approach presented here as a first step toward its application in real cells, where the concentrations of the biologically relevant components are not known *a priori*. Thus, we seek to infer free diffusion coefficients and kinetic parameters from the experiments without using any previous knowledge on the concentrations. In doing so, we not only derive the free diffusion coefficients that we are interested in but also quantify reaction rates. The approach involves performing sets of experiments for different concentration ratios so as to maximize the information that can be drawn from the data. In the present paper, we present a practical implementation for the case of Ca^{2+} and two single wavelength Ca^{2+} dyes. We show that, even if the free diffusion time of Ca^{2+}, being the lightest reactant, does not correspond to any of the characteristic decay times of the ACF, its value can be estimated by combining the various effective and free coefficients that can be quantified directly from the experiments without any previous knowledge of the concentrations involved. Although the transport of Ca^{2+} in the cytosol also involves the interaction with other (unobservable) species, we think that the approach presented here establishes a layout on how to advance towards its quantification in intact cells. We thus expect to be helping obtain reliable estimates of parameters that are key to determine the propagation range of the signals and to infer from their images the underlying Ca^{2+} distributions.

In order to advance with the practical implementation presented here, we first study theoretically the behavior of the ACF for the case of Ca^{2+} and a single wavelength dye analyzing with numerical simulations the applicability of an analytic approximation that is valid when the reaction timescale is small enough. We then show the results of a series of FCS experiments performed in aqueous solutions containing Ca^{2+} and different amounts of the Ca^{2+} indicator Fluo4 dextran both in its high and low affinity versions (Invitrogen-Molecular Probes, Carlsbad, CA). Fitting the observed ACF by the analytic approximation we corroborate the validity of the approximations and derive diffusion coefficients and the off-rate of the Ca^{2+}-dye binding reaction, in solution. A similar approach can be used to characterize the kinetic properties of other Ca^{2+} dyes. As we mentioned before, our final aim is to be able to apply a similar approach to experiments performed in intact cells. As a preliminary step we here obtain an estimate of the free diffusion coefficients of Ca^{2+} and its dyes in the cytosol of *Xenopus laevis* oocytes by assuming that they only differ from those derived in solution due to differences in viscosity between both media. Thus, we assume that the ratio between the free diffusion coefficients of any two substances remains the same in both settings. In this way, by solely quantifying the rate of diffusion of a molecule that diffuses freely in the cytosol and in solution we can infer the free diffusion coefficient of Ca^{2+} and the dyes in the cytosol as well. We present such quantification in the Appendix. Thus, the practical implementation presented in this paper not only highlights the advantages of our approach but it also allows us to derive a preliminary estimate of a parameter that is key to quantify the free Ca^{2+} distribution that underlies a Ca^{2+} image.

Ca^{2+} signals are not the only example in which being able to tell apart the contributions of free diffusion and reactions on the net transport rate of labeled substances is relevant. We have recently shown [21] the necessity of going beyond the description of effective coefficients to interpret correctly the apparently disparate estimates of the protein, Bicoid, diffusion coefficient derived from FCS [22] and fluorescence recovery after photobleaching (FRAP) [23] experiments. This example also shows that the comprehensive quantifiable description of a physiological process requires having a biophysical model for the dynamics of the relevant concentrations that depends on concentration-independent biophysical parameters. It is via such a model that the response of the system over time in front of different stimuli can be predicted. Being able to derive estimates of the concentration-free biophysical parameters *in situ* is thus relevant to achieve a meaningful description. The approach presented in this paper can be adapted and applied to other problems. Therefore, its relevance goes beyond quantifying the biophysical parameters associated to Ca^{2+} and its dyes.

II. MATERIALS AND METHODS

A. FCS Theory

Fluorescence correlation spectroscopy (FCS) monitors the fluctuation of the fluorescence in a small volume. Fluctuations

TABLE I. Aqueous solutions probed with FCS experiments. They also contain 100 mM KCl and 30 mM MOPS at pH 7.2.

Fluo4 high affinity			Fluo4 low affinity		
Aqueous solution	Ca^{2+}_{tot}(nM)	$[F4]_{tot}$(nM)	Aqueous solution	Ca^{2+}_{tot}(nM)	$[F4]_{tot}$(nM)
1	4285	429	10	4285	214
2	4285	857	11	4285	429
3	4285	1371	12	4285	857
4	4285	1886	13	4285	1114
5	4285	2571	14	4285	1371
6	4285	4286	15	4285	1886
7	4285	9000	16	4285	2571
8	4285	15 000	17	4285	4286
9	4285	19 286	18	4285	9000

are characterized by the time-averaged autocorrelation function (ACF), which is defined as

$$G(\tau) = \frac{\langle \delta f(t) \delta f(t+\tau) \rangle}{\langle f(t) \rangle^2}, \tag{1}$$

where $\langle f(t) \rangle$ is the average fluorescence in the sampling volume and $\delta f(t)$ is the deviation with respect to this mean at each time, t. As explained in the Appendix, when the fluorescence comes from a single species, P_f, that diffuses freely with coefficient D_f (i.e., does not react), the ACF is of the form

$$G(\tau) = \frac{g}{\left(1+\frac{\tau}{\tau_f}\right)\sqrt{1+\frac{\tau}{w^2\tau_f}}}, \tag{2}$$

where $w = w_z/w_r$ is the aspect ratio of the sampling volume and w_z and w_r are the sizes of the beam waist along z and r, with z the spatial coordinate along the beam propagation direction and r a radial coordinate in the perpendicular plane; the effective volume is $V_{ef} \equiv \pi^{3/2} w_r^2 w_z$; $\tau_f = w_r^2/(4D_f)$ is the characteristic time of diffusion of the particles across the sampling volume and $g = G(\tau = 0) = 1/(V_{ef} P_{tot})$, where P_{tot} is the particle concentration. When the dynamics of the fluorescent species is described by a reaction-diffusion model most often there is not a simple analytic expression for the ACF. It can always be written as a sum of integrals, each one associated to one of the branches of eigenvalues that rule the dynamics of the linearized reaction-diffusion equations of the model. Each of these integrals is called a "component" of the ACF. In the case of interest for the present paper, there are three relevant species: free Ca^{2+} (C), free dye (F), and Ca^{2+}-bound dye $[CF]$, which diffuse with free coefficients D_C (C) and D_F [F and $[CF]$] and react according to

$$C + F \underset{k_{on}}{\overset{k_{off}}{\leftrightarrows}} [CF], \tag{3}$$

with on- and off-rates, k_{on} and k_{off}, respectively. The corresponding (spatially uniform) equilibrium concentrations, C_{eq}, F_{eq}, and $[CF]_{eq}$ satisfy

$$[CF]_{eq} = \frac{C_{eq} F_{tot}}{C_{eq} + K_d}, \tag{4}$$

where $K_d = k_{off}/k_{on}$ and $F_{tot} = F_{eq} + [CF]_{eq}$ is the total dye concentration. There are three branches of eigenvalues for this system and the ACF then has three components. Simple algebraic expressions can be obtained for the components in certain limits. In particular, in this paper we present the results obtained in the "fast reaction limit" that holds when the characteristic time of the reaction Eq. (3) is shorter than the time it takes for the species to diffuse across the observation volume [i.e., if $\tau_{reac} \equiv [k_{off} + k_{on}(C_{eq} + F_{eq})]^{-1} < w_r^2/(4D_F)$]. For more details, see the Appendix, where we also compare the "full" (integral expression of the) ACF computed numerically with the analytic approximation derived in the fast reaction limit that is presented in the Results section and some of their components separately.

B. FCS Experiments

1. Aqueous solutions

Aqueous solutions were prepared with different concentrations of the Ca^{2+} indicator Fluo4 dextran high or low affinity (Invitrogen-Molecular Probes, Carlsbad, CA), employing the solutions of a Ca^{2+} calibration buffer kit (Invitrogen-Molecular Probes). Each solution contained 4.3 μM Ca^{2+}, 100 mM KCl, 30 mM MOPS, pH 7.2, and different concentrations of the Ca^{2+} indicator ranging from 200 nM to 9 μM and from 400 nM to 20 μM for the low and high affinity version, respectively. Four or five separate experiments were performed for each solution. Some of the results were finally discarded as explained later. The solutions that were probed and fitted are listed in Table I.

2. Acquisition

FCS measurements were performed on a spectral confocal scanning microscope FluoView 1000 (Olympus, Tokyo, Japan), employing a 60×, 1.35 N.A. oil-immersion objective (UPlanSAPO, Olympus) and a pinhole aperture of 115 μm. Single point measurements at a 50-kHz sampling rate were performed for a total duration of 167 s (equivalently, 8 365 312 data points) employing a 488-nm line and detecting the fluorescence in the range (500–600) nm. The measurements were performed at ∼20 μm from the coverslip.

3. Data analysis

Experimental ACFs were calculated with a custom-made routine written on the Matlab platform [24]. To this end, each 167-s-long record was divided into $N = 1021$, 164-ms-long

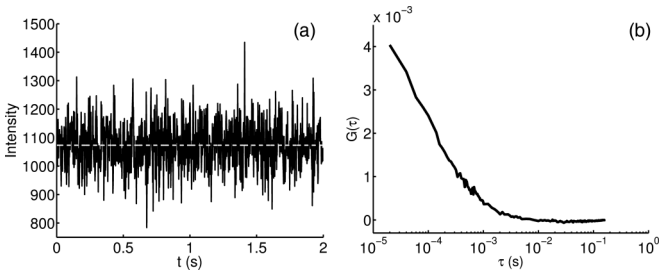

FIG. 1. Average ACF. (a) Typical stationary time-course of fluorescence fluctuations obtained from FCS measurements performed in aqueous solutions with Ca^{2+} and Fluo4 dextran. (b) Prototypical example of an average ACF.

segments containing 2^{13} points each for the experiments in aqueous solutions. The ACF was computed for each of the $N = 1021$ segments from which the average ACF was obtained. A prototypical example of an average ACF is shown in Fig. 1(a). About three experiments were performed for each set of concentrations of Table I. The respective ACFs were fitted separately. The biophysical parameters were derived from the fitting parameters obtained for each experiment. The average and the standard error of the mean (SEM) of the biophysical parameters were then computed over the values obtained for each experimental condition. We also computed averages and SEM over all experimental values, regardless of the condition, of those parameters that we expected to remain invariant in all experiments. Based on the theoretical calculations presented in the Results section, we fitted the average ACF by an expression of the form

$$G(\tau) = \frac{g}{\left(1+\frac{\tau}{\tau_0}\right)\sqrt{1+\frac{\tau}{w^2\tau_0}}} + \frac{g_1}{\left(1+\frac{\tau}{\tau_1}\right)\sqrt{1+\frac{\tau}{w^2\tau_1}}} + \frac{g_2 e^{-\nu\tau}}{\left(1+\frac{\tau}{\tau_2}\right)\sqrt{1+\frac{\tau}{w^2\tau_2}}}, \quad (5)$$

where $w = w_z/w_r$ is the aspect ratio of the sampling volume, as before, and the various times are related to diffusion coefficients by $\tau_i = w_r^2/(4D_i), i = 1,2,3$, with the beam waist, w_r. Only experiments for which the mean fluorescence in the observation volume remained approximately constant during the whole record were fitted. Experiments for which the average ACF was too noisy were also discarded. In all cases we tried to fit the experiments leaving all seven parameters of Eq. (5) (g, g_1, g_2, τ_0, τ_1, τ_2, ν) free to be fitted. In others, we set $g_2 = 0$ and only derived g, g_1, τ_0, and τ_1. Thus, we tried three and two component fits for each experiment. All fitting parameters were determined for each average ACF via a nonlinear least squares fit using the Matlab built-in function nlinfit. In the figures we show the average of the displayed fitting parameters and the average error computed over all the experiments in a given set.

4. Characterization of the confocal volume

The radial beam waist and the aspect ratio were determined to be w_r=0.262–0.292 μm and $w = w_z/w_r = 5$ by measuring the translational three-dimensional diffusion of fluorescein (Sigma, St. Louis, MO) at 100 nM in buffer solution pH 9, assuming a diffusion coefficient of 425 $\mu m^2/s$ [25]. Thus, the resulting effective volume was V_{ef}= (0.59 ± 0.1) μm^3.

III. RESULTS

A. Theoretical ACF for a solution with Ca^{2+} and a single wavelength dye in the limit of fast reactions.

In the fast reaction limit, the ACF for a solution of Ca^{2+} and a single wavelength dye can be approximated by [17,20] (see Appendix):

$$G_{\text{approx}}(\tau) = G_F(\tau) + G_{ef1}(\tau) + G_{ef2}(\tau), \quad (6)$$

$$G_F(\tau) = \frac{g_F}{\left(1+\frac{\tau}{\tau_F}\right)\sqrt{1+\frac{\tau}{w^2\tau_F}}}, \quad (7)$$

$$G_{\text{ef1}}(\tau) = \frac{g_{\text{ef1}}}{\left(1+\frac{\tau}{\tau_{\text{ef1}}}\right)\sqrt{1+\frac{\tau}{w^2\tau_{\text{ef1}}}}}, \quad (8)$$

$$G_{\text{ef2}}(\tau) = \frac{g_{\text{ef2}} e^{-\nu_F\tau}}{\left(1+\frac{\tau}{\tau_{\text{ef2}}}\right)\sqrt{1+\frac{\tau}{w^2\tau_{\text{ef2}}}}}, \quad (9)$$

where $\tau_F = w_r^2/(4D_F)$ and $\tau_{\text{ef}i} = w_r^2/(4D_{\text{ef}i})$, $i = 1,2$, with

$$D_{\text{ef1}} = \frac{D_C + \alpha D_F}{1+\alpha}, \quad (10)$$

$$D_{\text{ef2}} = \frac{\alpha D_C + D_F}{1+\alpha}, \quad (11)$$

and $\alpha = \frac{F_{\text{eq}}^2}{F_{\text{tot}} K_d}$, and

$$\nu_F = k_{\text{off}}\left(1 + \frac{F_{\text{eq}} + C_{\text{eq}}}{K_d}\right). \quad (12)$$

The weights g_F, g_{ef1}, and g_{ef2} are given by

$$g_F = \frac{1}{V_{\text{ef}} F_{\text{tot}}}, \quad (13)$$

$$g_{\text{ef1}} = \frac{1}{V_{\text{ef}}[CF]_{\text{eq}}} \frac{F_{\text{eq}}^2}{F_{\text{tot}} K_d} \frac{K_d}{(K_d + F_{\text{eq}} + C_{\text{eq}})}, \quad (14)$$

$$g_{\text{ef2}} = \frac{1}{V_{\text{ef}}[CF]_{\text{eq}}} \frac{K_d}{(K_d + F_{\text{eq}} + C_{\text{eq}})}. \quad (15)$$

Taking into account the equilibrium conditions Eq. (3) and $k_{\text{on}} C_{\text{eq}} F_{\text{eq}} = k_{\text{off}}[CF]_{\text{eq}}$, it can be shown that the sum of all the weights is inversely proportional to the concentration of fluorescent particles:

$$g_{\text{tot}} = g_{\text{ef1}} + g_{\text{ef2}} + g_F = \frac{1}{V_{\text{ef}}[CF]_{\text{eq}}}. \quad (16)$$

The sum of the two effective diffusion coefficients satisfies

$$D_{\text{ef1}} + D_{\text{ef2}} = D_C + D_F. \quad (17)$$

As in Ref. [20], the approximate analytic expression of the ACF given by Eqs. (6)–(9) is always valid for large enough τ. The first term, however, is exact. Thus, we expect to be able to derive D_F from all FCS experiments, regardless of the conditions. The approximations of g_{ef1} and g_{ef2} are valid for all values of τ provided that $\tau_{\text{reac}} \equiv (k_{\text{off}} + k_{\text{on}}(C_{\text{eq}} + F_{\text{eq}}))^{-1} \ll w_r^2/(4D_C)$. As shown in Ref. [18], the approximation can

TABLE II. Parameters used to compute the full and approximated ACFs numerically. For the concentrations of dye we tried the values listed in Table I.

Parameter	Value	
w_r	0.28 μm	
w	5	
D_C	760 $\mu m^2/s$	
D_F	85 $\mu m^2/s$	
C_{tot}	4285 nM	
	High affinity Fluo4	Low affinity Fluo4
K_d	772 nM	2600 nM
k_{off}	80 s^{-1}	300 s^{-1}

still be valid even if both timescales are of the same order of magnitude. In the Appendix, we compute numerically the ACF with no approximations that corresponds to a reaction-diffusion system as the one probed experimentally in the following sections using the parameters of Table II and the concentrations of Table I. The difference squared [ε^2 in Eq. (A11)] between the "full" and the approximated [Eqs. (6)–(9)] ACFs is relatively small even outside the region of validity under which Eqs. (8) and (9) are derived. For low enough total dye concentration, F_{tot}, the two ACFs are indistinguishable because they are dominated by the term given by Eq. (7), which is exact. Increasing F_{tot} a region is reached where the discrepancy between them is maximum. This occurs for $F_{tot}\sim 6.3\ \mu$M and $F_{tot}\sim 3.6\ \mu$M in the cases of high and low affinity Fluo4, respectively. ε^2 never exceeds $5.5\,10^{-9}$. If we compute χ^2/n, instead of Eq. (A11) we obtain values that never exceed 10^{-6} for the range of dyes concentrations used in the experiments. This is smaller than the values obtained when fitting the experimental data ($\sim 8\,10^{-6}$–$7\,10^{-4}$). Finally, the differences between both ACFs decrease as F_{tot} is further increased and the fast reaction approximation starts to hold for all time lags, τ. The other two properties of the ACF that always hold are those given by Eqs. (13) and (16), although the former should be considered with care due to uncertainties in the determination of individual weights from the fits. Equation (17) provides another useful relationship. As we show in what follows, the effective coefficients derived from the fits to the experimental ACF tend to satisfy this relationship even though their individual values may not correspond to those given by Eqs. (10) and (11). Thus, their sum can be used to quantify D_C once the free coefficient, D_F, is estimated.

Based on the above discussion we propose the following approach. First, perform a series of experiments of the same reaction-diffusion system varying the concentration of one of the reactants. In the experimental implementation presented here, we vary the concentration of the dye (see Table I). Once the experimental ACFs for each concentration in the series are determined, fit them using Eq. (5). This gives seven fitting parameters, g, g_1, g_2, τ_0, τ_1, τ_2, ν, for each concentration. From the analysis of the dependence of the timescales, τ_0 and τ_1, with the varying concentration, identify the one that remains invariant with the diffusive timescale of the dye, τ_F. This immediately implies the identification $\tau_{ef1}=\tau_1$ and $\tau_{ef2}=\tau_2$, which can be further validated by comparing the concentration dependence of τ_1 and τ_2 with what is expected of τ_{ef1} and τ_{ef2} for the system under study (while τ_{ef1} decreases with F_{tot}, τ_{ef2} increases). Derive the free diffusion coefficient of the dye, D_F, from $\tau_0=\tau_F=w_r^2/(4D_F)$. Since we will have as many values as concentrations probed, an average over all those values can be performed. Compute the diffusion coefficients, D_1 and D_2, from the fitting parameters, τ_1 and τ_2 using $\tau_i=\tau_{efi}=w_r^2/(4D_i)$. Assuming that they correspond to D_{ef1} and D_{ef2} so that they satisfy Eq. (17), compute their sum and analyze whether it remains approximately invariant for all concentrations probed. Average the sum over the values for which it remains invariant and equate it to D_C+D_F. From this equation, D_C can be derived. Identify the total weight derived from the fitting, $g+g_1+g_2$ with the expected total weight, g_{tot}, and compute $[CF]_{eq}$ from Eq. (16) for each solution probed experimentally. Equivalently, through the identification $g=g_F$, compute the total dye concentration, F_{tot}, using Eq. (13). Given these two concentrations, in principle it is possible to quantify the dissociation constant of the reaction from the concentration dependence of the two effective diffusion coefficients, D_{ef1} and D_{ef2}, derived from the fittings. Namely, D_{ef1} and D_{ef2} depend on the concentrations through the parameter $\alpha=F_{eq}^2/(F_{tot}K_d)$ [see Eqs. (10) and (11)] and F_{eq} can readily be computed as $F_{eq}=F_{tot}-[CF]_{eq}$. However, this would require that the timescales associated to the two effective diffusion coefficients be estimated with reasonable uncertainties, something that one can expect to happen only in the region of validity of the fast reaction approximation. Knowing the dissociation constant it is possible to derive the free Ca^{2+} concentration for each experiment using Eq. (4) and, with this and F_{tot}, the off rate from Eq. (12) identifying the fitting parameter, ν, with ν_F. In our experimental application we perform these computations using the dissociation constant that we derive from D_{ef2}. As we discuss later, in this way we obtain more reasonable values than using the dissociation constant provided by the vendor probably because the total concentrations of dye and Ca^{2+} that are actually in the experimental drop are not those that were inferred from the solution preparation. The approach proposed is illustrated in Fig. 1. Although it seems pretty straightforward, its practical implementation may carry a series of problems that we discuss in what follows. We also analyze to what extent the various biophysical parameters of the problem under study can be quantified as proposed.

B. Fitting parameters from FCS experiments in aqueous solutions with Ca^{2+} and Fluo4 dextran

In this section we show how we proceed to analyze the experimental data. In particular, we show the results of using Eq. (5) to fit the ACFs obtained from the set of experiments of Table I performed with Fluo4 high and low affinity. The fitting parameters are g, g_1, g_2, ν and the characteristic times τ_0, τ_1, and τ_2 from which we derive three diffusion coefficients D_0, D_1, and D_2 as explained before. Figure 2 shows the diffusion coefficients obtained in this way as a function of the total concentration of the dye used in the solutions, $[F4]_{tot}$, for high affinity [Fig. 2(a)] and low affinity [Fig. 2(b)] Fluo4. The open symbols correspond to the average and the error bars to the SEM computed over the values obtained for the various experiments performed under the same conditions that

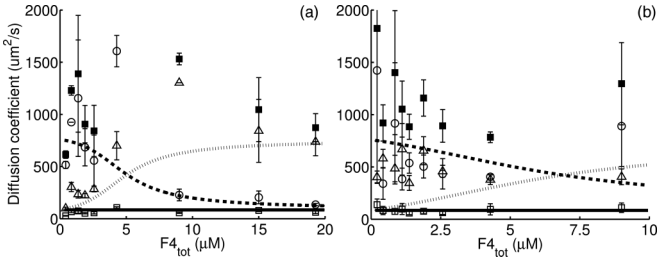

FIG. 2. Diffusion coefficients obtained from the fitting of the experimental data using Eq. (5), D_0 (open squares), D_1 (circles), D_2 (triangles), and the sum, $D_1 + D_2$ (solid squares), as functions of the total calcium dye concentration of the aqueous solutions, $[F4]_{\text{tot}}$. In solid line, $D_F = 85\,\mu\text{m}^2/\text{s}$, and in dash lines expected effective diffusion coefficients, D_{ef1} (bold) and D_{ef2} (light) given by Eqs. (10) and (11), respectively, with the calcium and dye concentrations employed in the aqueous solutions, $D_{\text{Ca}} = 760\,\mu\text{m}^2/\text{s}$, $D_F = 85\,\mu\text{m}^2/\text{s}$ and the dissociation constant given by the manufacturer, $K_d = 772$ nM and 2600 nM for high (a) and low (b) affinity Fluo4.

could be fitted. The solid squares correspond to the sum, D_1 and D_2. We also plot with curves the expected free diffusion coefficient of the dye, $D_F = 85\ \mu\text{m}^2/\text{s}$ [26] (solid line), and effective diffusion coefficients, D_{ef1} (bold dashed line) and D_{ef2} (light dashed line), calculated using Eqs. (10) and (11), with the dissociation constant given by the manufacturer ($K_d =$ 772 nM for high affinity and $K_d = 2600$ nM for low affinity), $D_C = 760\ \mu\text{m}^2/\text{s}$ [27], $D_F = 85\mu\text{m}^2/\text{s}$, and the total calcium and dye concentrations employed in the solutions.

The identification between the fitting parameters, g, D_0, g_1, D_1, g_2, D_2, ν, and the seven quantities, g_F, D_F, g_{ef1}, D_{ef1}, g_{ef2}, D_{ef2}, ν_F, of the theoretical formulas Eqs. (6)–(9) is immediate in the case of the last three, which correspond to the only component with an exponentially decaying term. For the other quantities it is not difficult to make the correspondence because $D_F < D_C$ implies that $D_F \leqslant D_{\text{ef1}}$. Furthermore, as may be observed in Fig. 2, there is one diffusion coefficient obtained from the fitting, D_0, that remains approximately invariant for all the analyzed concentrations. This should correspond to the free diffusion of the dye, D_F, which is concentration independent. In particular, the average and standard deviation computed over the means obtained for each experimental condition give $\langle D_0\rangle = 65\,\mu\text{m}^2/\text{s}$, $\sigma_{D0} = 22\,\mu\text{m}^2/\text{s}$ for the high affinity dye and $\langle D_0\rangle = 89\,\mu\text{m}^2/\text{s}$, $\sigma_{D0} = 25\,\mu\text{m}^2/\text{s}$ for the low affinity one. The corresponding SEMs, $7\,\mu\text{m}^2/\text{s}$ and $8\,\mu\text{m}^2/\text{s}$, respectively, are about 10% of the average. The other two diffusion coefficients obtained from the fitting, D_1 and D_2, change more noticeably with the dye concentration. In particular, we obtain $\langle D_{\text{ef1}}\rangle = 419\,\mu\text{m}^2/\text{s}$, $\sigma_{D\text{ef1}} = 237\,\mu\text{m}^2/\text{s}$, $\langle D_{\text{ef2}}\rangle = 437\,\mu\text{m}^2/\text{s}$, $\sigma_{D\text{ef2}} = 331\,\mu\text{m}^2/\text{s}$ for the high affinity dye and $\langle D_{\text{ef1}}\rangle = 648\,\mu\text{m}^2/\text{s}$, $\sigma_{D\text{ef1}} = 359\,\mu\text{m}^2/\text{s}$, $\langle D_{\text{ef2}}\rangle = 487\,\mu\text{m}^2/\text{s}$, $\sigma_{D\text{ef2}} = 121\,\mu\text{m}^2/\text{s}$ for the low affinity one. We interpret them as effective diffusion coefficients. Making the identifications $D_1 = D_{\text{ef1}}$ and $D_2 = D_{\text{ef2}}$, we know that their lower and upper limits are the free diffusion coefficients of the dye, D_F, and of calcium, D_C, respectively. In fact, both D_1 and D_2 are larger than D_0. Furthermore, in Fig. 2(a), D_1 decreases with $[F4]_{\text{tot}}$, while D_2 increases similarly to their theoretical counterparts, D_{ef1} and D_{ef2}. This trend is not as clear in Fig. 2(b) as in Fig. 2(a). The numerical simulations of the Appendix, on the other hand, show that fitting the ACF with Eq. (5) can give fitting parameters, D_1 and D_2, that differ from the theoretical ones, D_{ef1} and D_{ef2} for certain concentration values. It is because of these uncertainties that we try not to use their individual values, but their sum, $D_1 + D_2$ (shown in Fig. 2 with solid squares) to derive biophysical parameters. We observe in Fig. 2(a) that, with the exception of the $[F4]_{\text{tot}}$ values for which, according to the simulations, it is hardest to determine diffusion coefficients other than the one associated to the dye ($[F4]_{\text{tot}} < 1\,\mu$M) or for which the performance of the fast reaction approximation is worst ($4\,\mu\text{M} < [F4]_{\text{tot}} < 10\,\mu$M), the sum remains relatively invariant with varying $[F4]_{\text{tot}}$. In order to determine solely from the experiments the range of $[F4]_{\text{tot}}$ values for which $D_1 + D_2$ does not vary much we proceed as follows. We compute the average, $\langle D_1 + D_2\rangle$, and standard deviation, σ_{D1+D2}, of the means obtained for each experiment type. If $\sigma_{D1+D2}/\langle D_1 + D_2\rangle > 0.2$, we discard the means that differ the most from the average and recompute the average and standard deviation. We repeat the procedure until $\sigma_{D1+D2}/\langle D_1 + D_2\rangle \leqslant 0.2$. In particular, if we keep all the data points of Fig. 2(a) we obtain $\langle D_1 + D_2\rangle = 1193\,\mu\text{m}^2/\text{s}$ and $\sigma_{D1+D2} = 507\,\mu\text{m}^2/\text{s}$ which transform into $\langle D_1 + D_2\rangle = 856\,\mu\text{m}^2/\text{s}$ and $\sigma_{D1+D2} = 156\,\mu\text{m}^2/\text{s}$ after the application of our iterative procedure. This procedure prescribes that the data points coming from the experiments with $[F4]_{\text{tot}} = 0.857$, 1.371, 4.286, and 9 μM need to be discarded. If we apply a similar procedure to the coefficient, D_0, we have to discard the data points with $[F4]_{\text{tot}} = 0.429$ and 4.286 μM and obtain $\langle D_0\rangle = 64\,\mu\text{m}^2/\text{s}$, $\sigma_{D0} = 10\,\mu\text{m}^2/\text{s}$, which do not differ much from the values obtained if all the data points are kept. This is an indication that D_0 can be determined quite accurately for the whole range of concentration values explored in the paper and that it can be safely identified with the free coefficient of the dye, D_F. If, on the other hand, we recompute the average and standard deviation of $\langle D_1$ and $D_2\rangle$ but keeping only the experiment types for which their sum remains approximately constant according to the iterative procedure we obtain: $\langle D_{\text{ef1}}\rangle = 668\,\mu\text{m}^2/\text{s}$, $\sigma_{D\text{ef1}} = 489\,\mu\text{m}^2/\text{s}$, $\langle D_{\text{ef2}}\rangle = 525\,\mu\text{m}^2/\text{s}$, $\sigma_{D\text{ef2}} = 395\,\mu\text{m}^2/\text{s}$. The large ratios between the standard deviation and the average are an indication that these coefficients do vary with $[F4]_{\text{tot}}$ and, thus, correspond to effective rather than free coefficients. Applying the iterative procedure to the coefficient, D_0, of Fig. 2(b) we have to discard the results of the experiments with $[F4]_{\text{tot}} = 0.214$ and 9 μM and obtain $\langle D_0\rangle = 78\,\mu\text{m}^2/\text{s}$ and $\sigma_{D0} = 15\,\mu\text{m}^2/\text{s}$, which are also similar to the values obtained keeping all the data. Applying the procedure to the sum, $\langle D_1 + D_2\rangle$, we have to discard the results of the experiments with $[F4]_{\text{tot}} = 0.214$ and 0.857 μM and obtain $\langle D_1 + D_2\rangle = 998$, $\sigma_{D1+D2} = 180\,\mu\text{m}^2/\text{s}$. Discarding the same experiment types we obtain $\langle D_{\text{ef1}}\rangle = 500\,\mu\text{m}^2/\text{s}$, $\sigma_{D\text{ef1}} = 185\,\mu\text{m}^2/\text{s}$, $\langle D_{\text{ef2}}\rangle = 500\,\mu\text{m}^2/\text{s}$, $\sigma_{D\text{ef2}} = 134\,\mu\text{m}^2/\text{s}$ for the individual coefficients. In this case, the ratios between the standard deviation and the average are smaller than for the high affinity dye but are still larger than those of the sum. Taking all of this into account, we do make the identification $D_1 = D_{\text{ef1}}$ and $D_2 = D_{\text{ef2}}$ for both types of experiments for the concentration values for which the iterative procedure prescribes that their sum remains approximately invariant.

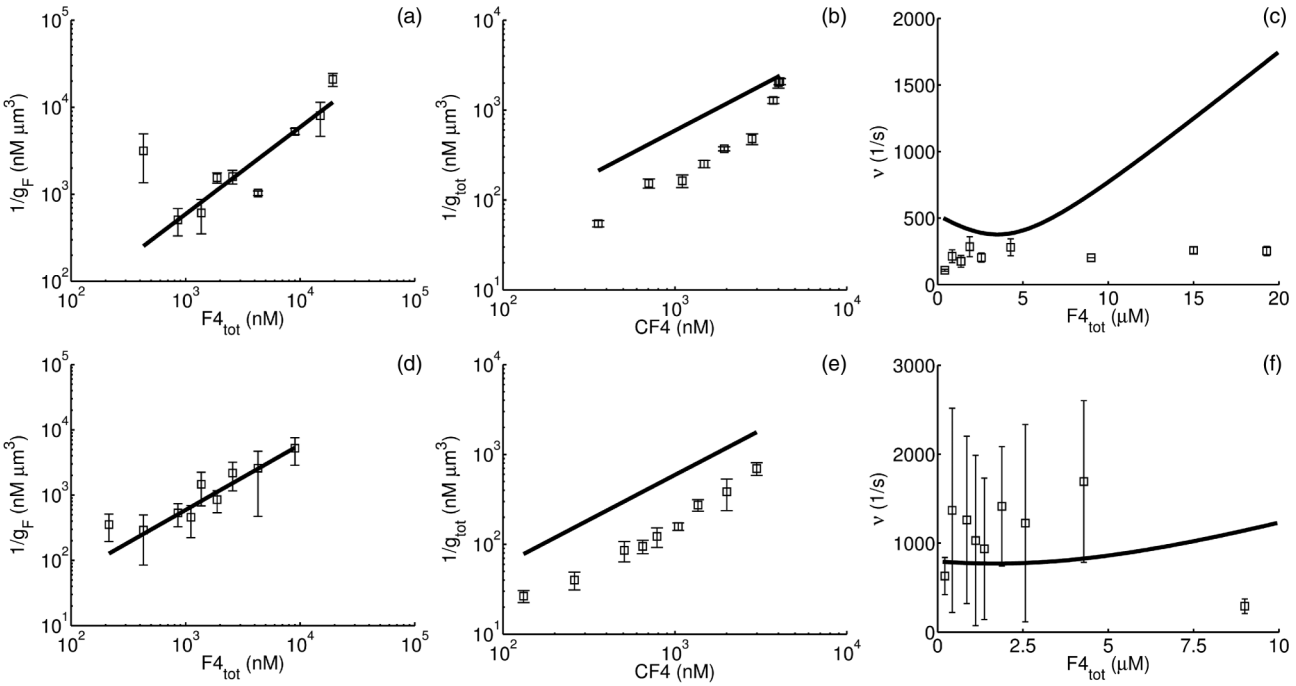

FIG. 3. Parameters derived from the fitting of the experimental ACFs (with symbols) and theoretical expected values (solid curves) computed using the concentrations of Table I and the dissociation constants of Table II. (a, d) Inverse of g_F as function of the total dye concentration used in the solutions, $[F4]_{\text{tot}}$. (b, e) Inverse of the sum of all the weights, g_{tot}, as function of the Ca^{2+}-bound dye concentration, $[CF4]$, computed theoretically setting $[CF4] = [CF]_{\text{eq}}$ and $F_{\text{tot}} = [F4]_{\text{tot}}$ in Eq. (4) with the constant, K_d, given by the manufacturer (Table II) and $C_{\text{tot}}^{(s)} = [CF4] + C_{\text{eq}}$ with $C_{\text{tot}}^{(s)}$ and $[F4]_{\text{tot}}$, the total concentrations of Table I. (c, f) ν as function of the total dye concentration used in the solutions, $[F4]_{\text{tot}}$. (a, b, c) correspond to experiments with Fluo4 high affinity and (d, e, f) with Fluo4 low affinity.

We now test to what extent two of the weights derived from the fitting depend on the concentrations used to make the solutions as predicted by the theory. We do it with the two weights that do not involve any approximation and that would be used to derive concentrations in case they were unknown: the total weight, g_{tot}, and the one that we identify with νg_F. We show in Figs. 3(a), and 3(d) the inverse of the latter as functions of the total dye concentration used in the solutions, $[F4]_{\text{tot}}$, for high and low affinity Fluo4, respectively, with symbols. Superimposed are the curves of the expected values computed using Eq. (13) with the concentrations of Table I and the observation volume derived from the calibration. Figures 3(b) and 3(e) are analogous to Figs. 3(a) and 3(d), respectively, but for the total weight as functions of the Ca^{2+}-bound dye concentration, $[CF4]$, computed with the same parameters as in Figs. 3(a) and 3(d) and the dissociation constants provided by the vendor (listed in Table II). In this case the theoretical expression is computed using Eq. (16). We use a logarithmic scale to compare the scaling of the different quantities with the varying concentration. In particular, we observe in Figs. 3(a) and 3(d) that the experimental values scale as $1/[F4]_{\text{tot}}$ as predicted by the theory [see Eq. (13)]. If we fit the experimental results using the values, $[F4]_{\text{tot}}$, determined by construction of the solution, the effective volume, V_{ef}, can be obtained from the fitting. Considering the inverse of g_F versus $[F4]_{\text{tot}}$, we found expected values ($V_{\text{ef}} = (0.54 \pm 0.08)\ \mu\text{m}^3$ and $V_{\text{ef}} = (0.56 \pm 0.08)\ \mu\text{m}^3$ for high affinity and low affinity Fluo4, respectively) that are consistent with the one obtained from the calibration ($V_{\text{ef}} = (0.59 \pm 0.1)\ \mu\text{m}^3$). Analogously, the experimental values displayed in Figs. 3(b) and 3(e) also scale with the Ca^{2+}-bound dye concentration as predicted by the theory [Eq. (16)], but there is a mismatch in the ordinate. As before, we can fit the experimental results using the equilibrium values, $[CF4]$, derived from the concentrations used in the solutions and the dissociation constant provided by the vendor. Considering the inverse of g_{tot} versus $[CF4]$ and fitting with a linear relation, the effective volume inferred was $(0.23 \pm 0.02)\ \mu\text{m}^3$ for Fluo4 high affinity and $(0.17 \pm 0.01)\ \mu\text{m}^3$ for the low affinity version of the dye, which are lower than the one obtained from the calibration ($V_{\text{ef}} = (0.59 \pm 0.1)\ \mu\text{m}^3$). We discuss later possible causes for this mismatch.

Finally, we show the values of ν_F derived from the fitting and the theoretical curve obtained using the fast reaction approximation, Eqs. (6)–(9), as a function of $[F4]_{\text{tot}}$ for high affinity [Fig. 3(c)] and low affinity [Fig. 3(f)] Fluo4. The experimental values were derived using our experimentally estimated concentrations and dissociation constant. There we observe that the values obtained for low $[F4]_{\text{tot}}$ concentrations are the ones that can be associated to the theoretical expression [Eq. (12)] from which an estimate of k_{off} can be derived. In order to estimate k_{off}, however, we used all the data available as explained in the Discussion.

C. Using the theory to determine free diffusion coefficients and reaction rates from the fitting

Being able to identify the parameters of the fitting with those of the theoretical ACF, Eqs. (6)–(9), allow us to go further

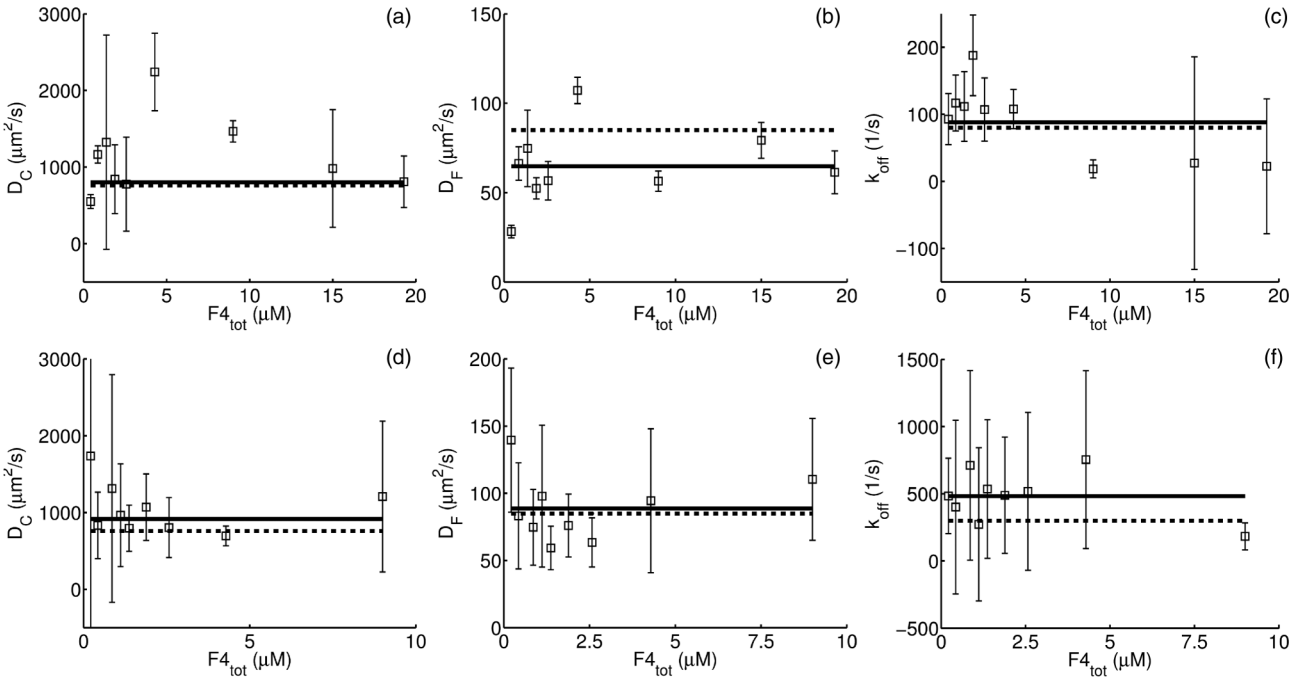

FIG. 4. Parameters of the underlying biophysical model derived from the fitting parameters for each aqueous solution, D_C, D_F, and k_{off} (mean and SEM over two or three experiments with one or two fits) and average of the values obtained for all experiment types in the case of D_F and k_{off} and only those for which the sum $D_1 + D_2$ remains invariant in the case of D_C (solid line), see Table III. (a, b, c) Fluo4 high affinity and (d, e, f) Fluo4 low affinity. In all cases we include the expected values (dashed line) based on the total concentrations used in the solutions and on the previous estimates of Table II.

and to quantify some relevant parameters of the underlying biophysical model for each aqueous solution, such as the free Ca^{2+} diffusion coefficient. This entails solving an overdetermined problem (seven equations with six unknowns). Based on the numerical exploration of the Appendix and the discussions presented before, we use the information given by g_F and g_{tot} and do not use g_{ef1} and g_{ef2} separately because these weights carry the largest errors. As already explained, knowing D_F, D_{ef1}, D_{ef2}, g_F, g_{tot}, and ν_F (which we identify with six of the seven parameters of the fitting) it is possible to infer the off-rate, k_{off}, and the dissociation constant, K_d, of the Ca^{2+}-dye reaction, the total dye concentration, F_{tot}, the Ca^{2+}-bound dye concentration, $[CF]_{\text{eq}}$, and the free diffusion coefficients, D_C and D_F. We show in Fig. 4 the values, D_C, D_F, and k_{off}, obtained as functions of the total dye concentration used in the aqueous solutions, $[F4]_{\text{tot}}$, both for the high affinity [Figs. 4(a)–4(c)] and the low affinity [Figs. 4(d)–(f)] versions of the dye. The symbols correspond to the values derived from the averages of the fitting parameters and the error bars are obtained via error propagation of the range of allowed fitting parameter values determined experimentally. This is why the final ranges embrace negative values that have no physical meaning but which reflect that the corresponding parameter is determined with a large uncertainty. The values, D_C, were computed as $D_1 + D_2 - \langle D_0 \rangle$ with the latter calculated over the means of all the experiment types. Since the solutions only differed in the total amount of dye k_{off}, D_C and D_F should remain approximately constant for all solutions. Based on our discussion on the behavior of the sum, $D_1 + D_2$, we expect D_C to be poorly determined for the experiment types for which $D_1 + D_2$ does not remain invariant and cannot be identified with $D_{\text{ef1}} + D_{\text{ef2}}$. If we drop the values, D_C, derived from the experiment types that should be discarded according to the application of the iterative procedure to the sum, $D_1 + D_2$, we obtain $D_C = (801 \pm 70)\ \mu\text{m}^2/\text{s}$ and $D_C = (915 \pm 68)\ \mu\text{m}^2/\text{s}$ for Fluo4 high and low affinity, respectively.

IV. DISCUSSION AND CONCLUSIONS

In this work we have shown how free diffusion coefficients, reaction rates, and concentrations can be quantified in reaction-diffusion systems by performing sets of FCS experiments in different conditions and using a biophysical model to interpret the experimental results. In particular, we have applied this approach to the case of Ca^{2+} and a single wavelength Ca^{2+} dye. Given that we can only monitor the fluorescence of the dye, which increases by over an order of magnitude upon Ca^{2+} binding, the only way to study Ca^{2+} diffusion with this technique is by allowing that several reactions between Ca^{2+} and the dye occur within the observation volume. To analyze the experiments we computed an approximated (analytic) expression of the fluorescence fluctuations ACF that is valid for fast reaction timescales and analyzed numerically its limits of applicability. We then performed a series of experiments in solutions containing Ca^{2+} and the Ca^{2+} dye Fluo4 dextran (both high and low affinity) with which we validated the approach and established its limitations. This application showed, among other things, that the ACF could be used outside its limits of applicability to extract reliable information on certain parameters. The analysis of the experiments yielded estimates of the free diffusion coefficients of Ca^{2+}, of two single wavelength Ca^{2+} dyes (high and low affinity Fluo4)

TABLE III. Parameters estimated with our model from FCS experiments performed with high and low affinity Fluo4 (HAF4 and LAF4, respectively). Results are expressed as mean ± SEM.

Parameters	Our estimates (HAF4)	Our estimates (LAF4)	Previous estimates
D_F	(65±7) $\mu m^2/s$	(89±8) $\mu m^2/s$	85 $\mu m^2/s$ [26]
D_C	(801±70) $\mu m^2/s$	(915±68) $\mu m^2/s$	760 $\mu m^2/s$ [27]
k_{off}	(88±19) 1/s	(483±61) 1/s	

and of the reaction rates between them, all of them in aqueous solution. Although the free diffusion coefficient of Ca^{2+} is already well known ($D_C \sim$ (750–800) $\mu m^2/s$ [27,28]), being able to derive it from the observation of a system in which it is not diffusing freely is quite relevant and provides hints on how to proceed in other settings. Addressing fundamental problems in Ca^{2+} signaling requires the combination of experiments and modeling for which quantifying key biophysical parameters, such as the Ca^{2+} diffusion coefficient, *in situ*, is most relevant [29]. Optical techniques are ideal to probe intracellular transport with minimum disruption [30]. Measuring intracellular Ca^{2+} transport in this way, however, is not straightforward because of the multiple interactions of the ions with different cell components [31,32] and because Ca^{2+} dyes are also Ca^{2+} buffers that alter the ions transport rate [33]. The quantification of diffusion coefficients and reaction constants in such a case requires a careful interpretation of the experimental data in terms of an underlying biophysical model [21]. The work contained in this paper constitutes a necessary first step to advance in this direction.

The approximation of the ACF [Eqs. (6)–(9)] with which we analyzed the experimental data had been used previously to study other systems [17]. Our particular application highlights some of the differences with respect to these previous studies. In particular, Eq. (7) shows that the free diffusion coefficient of the massive molecule (the biologically relevant one in Ref. [17]) can readily be obtained from the ACF with no approximations. In our case, instead, the free diffusion coefficient of the biologically relevant substance (Ca^{2+}) only enters the ACF through the effective diffusion coefficients. We thus had to derive it from them. It is also important to note that, in the limit opposite to the fast reaction one, the ACF is characterized only by the free coefficients of the fluorescent substances [18] (and by reaction rates if some of them are immobile [19]). In this regard, the case of Ca^{2+} and its dyes is different from the situation of a fluorescent protein that interacts with immobile or slowly moving binding sites studied in Refs. [20,21] for which reducing the observation volume (and, thus, the diffusion timescale) could be an option to quantify the free diffusion coefficient of the protein. The only possibility of withdrawing D_C from FCS experiments performed with Ca^{2+} dyes is then by working in conditions in which some of the correlation times depend on effective diffusion coefficients. The application presented in this paper shows that is not necessary to be well within the region where the reaction timescale is much smaller than the (free) diffusion one to be able to extract useful information from these coefficients. In particular, the fact that their sum has to remain constant for all dye concentrations provides a tool with which to probe the results and the key to derive D_C. In fact, the dye concentration values for which the sum departed the most from a constant (concentration independent) value approximately overlapped with those for which our numerical studies indicated that the difference between the approximated and the full ACFs was about maximal or that the estimates of the effective diffusion timescales could be poor because the ACF was dominated by the component associated to the free diffusion of the dye (see Figs. 4 and 6). Variations in the estimate of the free diffusion of the dye also allowed us to pinpoint the concentration range for which the fast reaction approximation was not good. In this way, solely based on the experimental observations we derived estimates of the free diffusion coefficients of the dyes (58–97 $\mu m^2/s$) and of Ca^{2+} (731–983 $\mu m^2/s$) that are consistent, respectively, with the value obtained in solution for the 10 kDa tetramethylrhodamine-dextran (TMR-D, 85 $\mu m^2/s$) [26] and with previously estimated values [27,28], see Table III. This indicates that even in the absence of an *a priori* theoretical study a relatively accurate value of the free diffusion coefficient of the dye and of its sum with the free diffusion coefficient of Ca^{2+} can be inferred from the experiments. The studies of Ref. [19], on the other hand, show that, given a finite time observation, it takes much longer for the individual weights than for the correlation times to converge to their expected (asymptotic) values. Based on these observations we concluded that in order to derive biophysical from fitting parameters it was best to work with the timescales associated to the free diffusion of the dye and the one that enters the exponential term, with the sum of the other two diffusion coefficients, with the weight that can be identified with g_F and with the total weight of the ACF. In any case, we also estimated the dissociation constant of the dye using one more fitting parameter. Using our estimated K_d gave more reasonable values than using the constant provided by the vendor. As discussed in what follows this might be due the fact that those quantities which estimates require knowing K_d depend on this constant through a ratio with respect to concentrations. It then seems that the errors in K_d and the estimated concentrations somehow cancel out.

Given the expected uncertainties in the determination of the weights, we performed a series of self-consistency checks on their behavior. The comparison of the total Fluo4 or the Ca^{2+}-bound dye concentration dependence of the inverse of the experimentally determined weights, g_F and g_{tot}, with the theoretical expressions, Eqs. (16) and (13) showed agreement between theory and experiment in the case of g_F [Figs. 3(a) and 3(d)] and a mismatch in that of g_{tot} [Figs. 3(b) and 3(e)]. Fitting the experimental points by a linear relationship between the inverse of g_F and $[F4]_{tot}$ we obtained (0.54 ± 0.08) μm^3 for high affinity and (0.56 ± 0.08) μm^3 for low affinity Fluo4, in good agreement with the experimentally calibrated volume, V_{ef}= (0.59 ± 0.1) μm^3. In the case of the

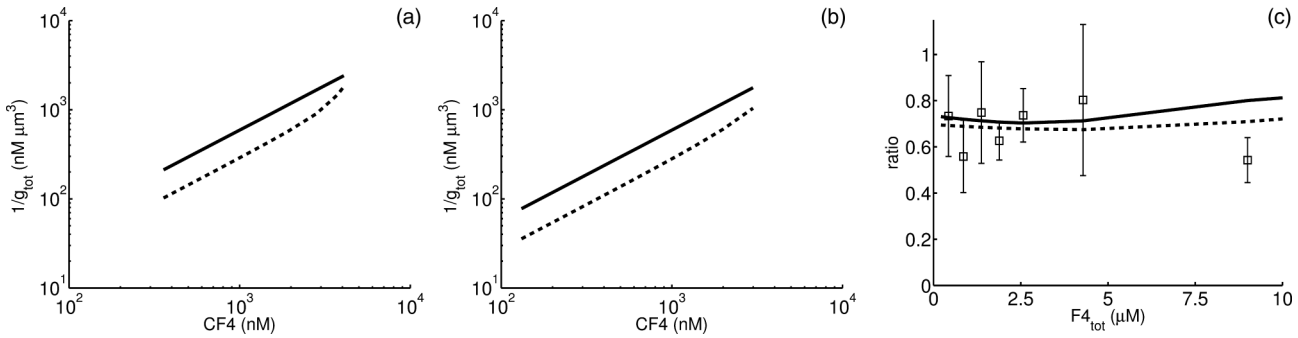

FIG. 5. (a) Inverse of the total weight of the ACF computed theoretically using the dissociation constant provided by the vendor, the effective volume of the calibration, $V_{ef} = 0.59\ \mu m^3$, and the total Ca^{2+} and dye concentrations of the experimental solutions ($V_{ef}[CF4]$, solid curve) or the fractions, $\zeta_C = 0.2$ and $\zeta_F = 0.5$, respectively, of those total concentrations ($V_{ef}[CF]_{eq}$, dashed curve) as functions of $[CF4]$ for the high affinity dye. (b) Similar to (a) but for the low affinity dye. (c) Ratio between the total weights, g_{tot} (circles), obtained in experiments with high and low affinity Fluo4 and ratios of the theoretical values, $[CF]_{eq}$(low)/ $[CF]_{eq}$(high) (dashed line) and $[CF4]$(low)/ $[CF4]$(high) (solid line), displayed in (a) and (b) as functions of the total dye concentration used to prepare the solutions, $[F4]_{tot}$.

inverse of g_{tot} versus $[CF]_{eq}$ relationship, the experimental points lied below the theoretical prediction, as if the actual concentrations of Ca^{2+}-bound dye were smaller than those that can be derived from Eq. (4) using the ones of the solutions and the dissociation constant provided by the vendor. If, as before, we fit the experimental points by a relationship between the inverse of g_{tot} and $[CF4]$ we obtain $(0.23 \pm 0.02)\ \mu m^3$ for high affinity and $(0.17 \pm 0.01)\ \mu m^3$ for low affinity Fluo4, which are smaller than the calibrated one. One possibility for the mismatch between the theoretically predicted curve and the experimental points in Figs. 3(b) and 3(e) is that part of the Ca^{2+} ions and/or of the dye molecules be trapped by the coverslip where the drop with the solution is placed. In fact, protein adsorption by the sample holder was argued to explain the differences observed in the pseudo-first-order reaction rates that could be estimated with FCS in Ref. [16]. If Ca^{2+} or the dye had been partially adsorbed by the glass in our experiments, then the actual total concentrations in the bulk of the drop, C_{tot} and F_{tot}, would have been different from those used to prepare the solutions, Ca^{2+}_{tot} and $[F4]_{tot}$. In such a case, g_{tot} would have been given by Eq. (16) with $[CF]_{eq}$ the actual Ca^{2+}-bound dye concentration in the bulk, not $[CF4]$, the one that can be computed using the concentrations employed in the solutions. We show in Figs. 5(a) and 5(b) plots of $V_{ef}[CF4]$ (solid lines) and $V_{ef}[CF]_{eq}$ (dashed line) as functions of $[CF4]$, for the high [in Fig. 5(a)] and the low [in Fig. 5(b)] affinity dyes. In both figures we computed $[CF]_{eq}$ under the assumption that the fractions, $\zeta_C = 0.8$ and $\zeta_F = 0.5$ of the total Ca^{2+} and dye concentrations of the solution, respectively, had been adsorbed by the coverslip. The dashed curves are similar to those of Figs. 3(b) and 3(e), in particular, they show the reduction of the mismatch with increasing $[F4]_{tot}$ observed in the experiments. Although glass adsorption could be playing a role, we must also recall that the relationship between g_{tot} and the Ca^{2+}-bound dye concentration also depends on the dissociation constant of the Ca^{2+}-dye reaction and that using larger K_d values would decrease the mismatch between the experimental points and the theoretical curve. In order to analyze to what extent the results obtained for both dyes agree with what can be expected theoretically based on the values of K_d provided by the vendor and on the concentrations used in the solutions we show in Fig. 5(c) the ratio of total weights obtained using each dye (weight for high over weight for low affinity Fluo4 with symbols) as a function of the total dye concentration for which we had experiments performed with both dyes. We also show

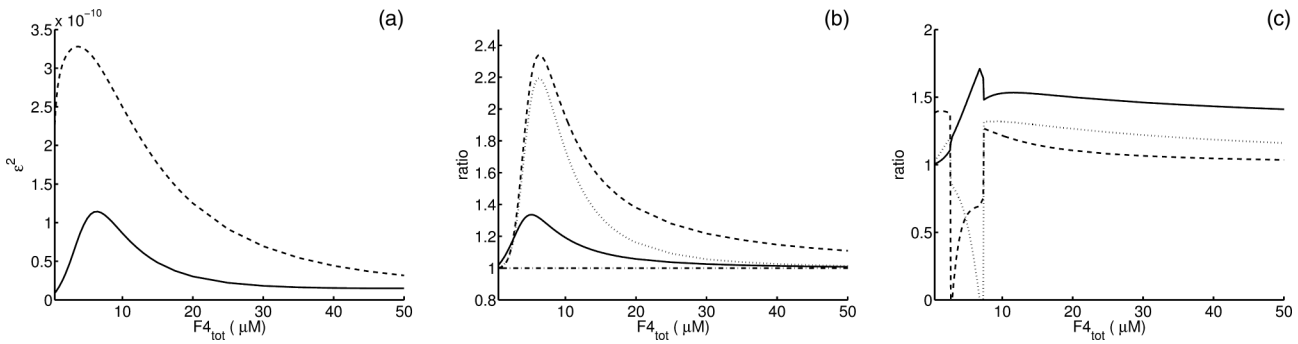

FIG. 6. (a) Difference between the full and approximated ACFs obtained using the parameters of Table II for Fluo4 high (solid line) and low (dashed line) affinity. (b) Ratios τ_0/τ_F (solid line), τ_1/τ_{ef1} (dashed line), τ_2/τ_{ef2} (dotted line), and ν_F/ν (dashed-dotted line) between fitting and fast reaction approximation times as functions of $[F4]_{tot}$ for high affinity Fluo4 when all parameters are free to fit in Eq. (5). (c) Similar to (b) but for the ratios between the fitted and the fast reaction weights, g/g_F (solid line), g_1/g_{ef1} (dashed line), g_2/g_{ef2} (dotted line), as functions of $[F4]_{tot}$ for Fluo4 high affinity when the timescales in Eq. (5) are fixed at the fast reaction approximation values.

in the figure the ratios of the values of $[CF]_{eq}$ (dashed) and of $[CF4]$ (solid) of Fig. 5(b) over those of Fig. 5(a). The theoretical and experimental ratios should be equal according to Eq. (16). We observe that they mostly agree regardless of whether we compute the ratio assuming Ca^{2+} and dye adsorption by the coverslip (dashed curve) or not (solid curve), although the former seems to provide a better description. Now, having a reduced total dye concentration in the experiment would also lead to a larger value of the weight, g_F, compared to the expected one and although the experimental points and the theory are slightly off, they only differ by about 10% on average [see Figs. 3(a) and 3(d)]. In any case, we do expect individual component weights to carry larger errors than the that of the total weight. Thus, it could be reasonable that the weight associated to the dye could be not completely accurate. Another possibility to explain the mismatch could be an error in the calibration of the effective volume. In particular, changing the concentrations could produce a change in the refractive index of the sample that would in turn change the volume where the light is focused [34–36]. Thus, experiments performed using different solutions could correspond to different values of the effective volume that was calibrated in a medium with fluorescein and no added Ca^{2+} or Ca^{2+} dye. The calibration was performed using 100 nM of fluorescein and the solutions listed in Table I had concentrations that were orders of magnitude larger. Given that water has a smaller refractive index than the immersion medium of the objective (oil) and refractive indices increase with increasing solute concentration [37], the mismatch between the indices of the sample and of the objective's immersion medium would decrease with increasing concentration. The illuminated volume could then, in principle, be smaller for the Ca^{2+} dye experiments than during the calibration. The change in refractive index within the concentrations explored in this paper, however, would be too small [37] to account for a factor of 2 difference between the calibrated volume and the one that we could derive by fitting the experimental points in Figs. 3(b) and 3(e) by a straight line. Based on this discussion we conclude that most probably adsorption by the coverslip is affecting the experimental results. It is reassuring to note, however, that such a problem would not be present in intact cells. On the other hand, the low sensitivity of the ratio depicted in Fig. 5(c) on changes in the total dye or Ca^{2+} concentrations within those probed experimentally suggests that errors in the determination of the concentrations or the dissociation constant could be smoothed out when taking ratios of these quantities. This could explain why we obtained more reasonable estimates of the off-rate, k_{off}, when using the dissociation constant and concentrations determined from the experiments than if we used the K_d provided by the vendor. As may be observed in Fig. 3, the comparison of the experimental and theoretical results in the case of the inverse of the exponential correlation time derived [ν and ν_F given by Eq. (9)] showed the values of ν seemed to display the correct behavior only for those solutions with the smallest dye concentrations.

In any case, applying the theory to all the experimental results regardless of $[F4]_{tot}$ gave values of k_{off} within the same order of magnitude [see Figs. 4(c) and 4(e)]. Using the average of these values we obtained $k_{off} = (88\pm19)\ s^{-1}$ and $k_{off} = (483\pm61)\ s^{-1}$ for the high and low affinity Fluo4, respectively. Using the dissociation constant provided by the manufacturer, we obtained $k^*_{off} = (49\pm12)\ s^{-1}$ and $k^*_{off} = (624\pm94)\ s^{-1}$ instead. We did use the dissociation constant of the vendor to derive the on rates as $k_{on} = k_{off}/K_d$. In this way, for the high and low affinity versions of the dye, we found similar values ($k_{on} = (0.114\pm0.025)\ nM^{-1}s^{-1}$ and $k_{on} = (0.186\pm0.023)\ nM^{-1}s^{-1}$, respectively). This is consistent with the fact that, in BAPTA (1,2-bis(o-aminophenoxy)ethane-N,N,N′,N′-tetraacetic acid) based calcium indicators, increasing values of K_d result from an increase in the dissociation rate constant and negligible or only modest decreases in the association rates [38,39].

It is important to note that, while concentrations at equilibrium do not depend on k_{off} and k_{on}, separately, but on $K_d = k_{off}/k_{on}$, their time evolution does. Therefore, the values of k_{off} and k_{on} affect the behavior of the observed Ca^{2+} signals and knowing them is absolutely necessary to infer the spatiotemporal distribution of free Ca^{2+} from the images [8,9]. Knowing the free diffusion coefficients of Ca^{2+} and its dyes in the cytosol is necessary as well for this purpose. The values derived in the Results section, however, correspond to coefficients in aqueous solution (Table III). Assuming that the differences in the free diffusion coefficients in solution and in the cytosol are due to differences in viscosity between both media, we may assume that the ratio between the free diffusion coefficients of any two substances remains the same in both settings. Thus, by quantifying the rate of diffusion of a molecule that diffuses freely in the cytosol and in solution, we can infer the free diffusion coefficient of Ca^{2+} and the dyes in the cytosol as well. A word of caution must be introduced here as to what the meaning of "free diffusion coefficients" is in the context of cells where the displacement of molecules and ions is spatially restricted. As discussed in various papers [40–42], one should talk about a variety of coefficients depending on the timescale over which mean displacements are computed. As shown in Ref. [42], while at the 25–100 nm scale molecules seem to diffuse at the same rates in cells and in aqueous solutions, while above 100 nm, although the transport is not purely diffusive, an estimate of its rate shows a threefold reduction. The effective diffusion coefficient of Eq. (10) corresponds to computing the mean displacement over yet larger time or spatial scales. The main difference between this effective coefficient and those that arise due to spatial restrictions is the concentration dependence of the former that derives from the fact that the rate of binding depends on the concentration of the diffusible substance. In that regard, the "free" coefficients that we can derive applying our approach to experiments performed in cells should be considered as the concentration-independent coefficients that describe the displacement of the substances within the timescale that can be resolved with the experimental setup. With this view in mind the results of FCS experiments performed in oocytes of *Xenopus laevis* using TMR-D that we present in the Appendix should be interpreted. Fitting the ACF by an expression of the form Eq. (2), we obtained $D_{TMR} = (27 \pm 1)\ \mu m^2/s$. Considering that the TMR-D diffusion coefficient in solution is $D_{TMR} = 85\ \mu m^2/s$ [26], we obtained $D_{TMR\text{-}D}(solution)/D_{TMR\text{-}D}(oocyte) \sim 3$. Assuming that $D_{TMR\text{-}D}(solution)/D_{TMR\text{-}D}(oocyte) \sim D_{free}(solution)/D_{free}(oocyte)$, where D_{free} stands for free diffusion coefficient of any substance, we can use the free transport

rates (in the sense mentioned before) of Ca^{2+} and of its dyes in solution to infer their values in the cytosol. We obtain $D_C \sim$ (244–290) $\mu m^2/s$ and $D_F \sim$ (19–24) $\mu m^2/s$ starting from the free diffusion coefficients in solution obtained in the experiments performed with high affinity Fluo4, see Table III. The values derived for D_C are of the same order of magnitude as the one obtained in cytosolic extracts [5], although the latter (220 $\mu m^2/s$) is below our lower bound. Even though the cytosolic values estimated here are preliminary and will be further tested with FCS experiments performed directly in oocytes, this slight mismatch could be due to the fact that the effective diffusion coefficient obtained in Ref. [5] is the single molecule one and a misinterpretation of its meaning could lead to an underestimation of the actual diffusion rate of Ca^{2+} [1]. This highlights the need of having an underlying biophysical model to interpret transport rates when diffusion and reactions are intermixed. It also shows how by changing the experimental conditions it is possible to quantify concentration-independent biophysical parameters in these systems as done, e.g., in Ref. [43] by varying the observation volume. We thus expect the approach presented here to be useful for the quantification of transport rates in other biologically relevant reaction-diffusion systems.

ACKNOWLEDGMENTS

We are thankful to Emiliano Perez Ipiña for having provided the code to compute the full ACF and to Lucia Lopez and Estefania Piegari for help with some of experiments. This research has been supported by UBA (UBACyT Grant No. 20020130100480BA) and ANPCyT (PICT Grant No. 2013-1301). L.S. and S.P.D. are members of Carrera del Investigador Científico (CONICET).

APPENDIX

1. FCS theory

a. *ACF for a system with freely diffusing particles*

When the fluorescence comes solely from a single type of particles, P_f, that diffuse freely with coefficient, D_f, the fluorescence is given by

$$f(t) = \int Q I(r)[P_f](r,t) d^3r, \tag{A1}$$

where $[P_f](r,t)$ is the particle concentration at time, t, and spatial point, r, the parameter, Q, takes into account the detection efficiency, the fluorescence quantum yield and the absorption cross-section at the wavelength of excitation of the fluorescence. The region from where the fluorescence comes from is commonly approximated by a three-dimensional Gaussian:

$$I(r) = I(0)\, e^{-\frac{2r^2}{w_r^2}}\, e^{-\frac{2z^2}{w_z^2}}, \tag{A2}$$

with z the spatial coordinate along the beam propagation direction, r a radial coordinate in the perpendicular plane, and w_z and w_r the sizes of the beam waist along z and r, respectively. In this case, there is an analytic expression for the ACF, which is given by Eq. (2). Fitting the ACF obtained from experiments by Eq. (2), two parameters can be determined: g and the characteristic time τ_f. A previous calibration of the geometric parameters of the sample volume is required in order to obtain D_f from τ_f. This is done performing the same experiments on a sample for which D_f is already known. Once w_r and w_z are determined, the unknown D_f can be estimated from the characteristic time τ_f and P_{tot} from g.

b. *"Full" ACF of a system with* Ca^{2+} *and a single wavelength dye*

The equations that describe the dynamics of Ca^{2+}, C, and a single wavelength dye, F, that react and diffuse as described in Sec. II are

$$\frac{\partial [C]}{\partial t} = D_C \nabla^2 [C] - k_{on}[C][F] + k_{off}[CF], \tag{A3}$$

$$\frac{\partial [CF]}{\partial t} = D_F \nabla^2 [CF] + k_{on}[C][F] - k_{off}[CF], \tag{A4}$$

$$\frac{\partial [F]}{\partial t} = D_F \nabla^2 [F] - k_{on}[C][F] + k_{off}[CF], \tag{A5}$$

In FCS experiments in aqueous solution containing Ca^{2+} and F it is assumed that both species are uniformly distributed and in equilibrium, so that their mean concentrations are given by the equilibrium concentrations C_{eq}, F_{eq} and $[CF]_{eq}$, that satisfy Eq. (4), $C_{eq} + [CF]_{eq} = C_{tot}$ and $F_{eq} + [CF]_{eq} = F_{tot}$. Neglecting the fluorescence from the Ca^{2+}-free dye, the fluorescence intensity is given by

$$f(t) = \int Q I(r)[[CF]](r,t) d^3r, \tag{A6}$$

with Q and I as before. As done in Sigaut *et al.* [20], we follow Krischevsky and Bonnet [44] to determine the spatiotemporal dependence of the fluorescence fluctuations in this case. Namely, the evolution Eqs. (A3)–(A5) are linearized around the equilibrium solution, Eq. (4). The solution of these linearized equations is then computed in Fourier space and written in terms of branches of eigenvalues, $\lambda(q)$, and eigenvectors, $\chi(q)$, with q the variable in Fourier space [conjugate to the spatial vector (r,z)]. The fluorescence fluctuations are then obtained as in Eq. (A6) but replacing $[CF]$ by the corresponding component of the solution of the linearized problem, $\delta[CF]$. The calculation of the ACF finally assumes that the correlation length of the concentrations at any given time is much smaller than the intermolecule distance and that the number of molecules obeys Poisson statistics so that its variance and its mean are equal. In this way the ACF, $G(\tau)$, can be written as a sum, $G(\tau) = G_{\lambda_F}(\tau) + G_{\lambda_1}(\tau) + G_{\lambda_2}(\tau)$, of as many components as branches of eigenvalues of the linearized problem with $G_{\lambda_F}(\tau)$ given by Eq. (7) and

$$G_{\lambda_1}(\tau) = \frac{1}{2(2\pi)^3 h [CF]_{eq}} \int d^3q\, I(q) \left[1 + \frac{(a-h)\nu_F}{(a+h)\Psi(q)} + \frac{(D_C - D_F)q^2}{\Psi(q)} \right] e^{\lambda_1 t}, \tag{A7}$$

$$G_{\lambda_2}(\tau) = \frac{1}{2(2\pi)^3 h [CF]_{eq}} \int d^3q\, I(q) \left[-1 - \frac{(a-h)\nu_F}{(a+h)\Psi(q)} + \frac{(D_C - D_F)q^2}{\Psi(q)} \right] e^{\lambda_2 t}, \tag{A8}$$

where $I(q) = \exp[-(w_r^2 q_r^2 + w_z^2 q_z^2)/4]$, q_r and q_z are the Fourier coordinates conjugated to the radial and axial coordinates, r and z, respectively, $a = F_{eq}/K_d$, $h = F_T/F_{eq}$, $\nu_F = k_{off}(a+h)$, $\Psi(q) = \sqrt{(D_F - D_C)^2 q^4 + 2q^2(D_F - D_C)(h-a)k_{off} + (h+a)^2 k_{off}^2}$ and the eigenvalues:

$$\lambda_1 = -\frac{1}{2}[k_{off}(a+h) + (D_F + D_C)q^2] + \frac{\Psi}{2}, \tag{A9}$$

$$\lambda_2 = -\frac{1}{2}[k_{off}(a+h) + (D_F + D_C)q^2] - \frac{\Psi}{2}. \tag{A10}$$

c. *Approximated ACF of a system with* Ca^{2+} *and a single wavelength dye*

Although $G_{\lambda_1}(\tau)$ and $G_{\lambda_2}(\tau)$ can be computed numerically, in general there is no analytic algebraic expression for these two components as there is for the one that corresponds to the branch of eigenvalues, $\lambda_F = -D_F q^2$, associated to the free diffusion coefficient of the dye, D_F [see Eq. (7)]. As done in Ref. [20] an analytic expression for $G_{\lambda_1}(\tau)$ and $G_{\lambda_2}(\tau)$ and, consequently, for the ACF can be obtained in the limit of small q which is always valid for long enough times, τ. Expanding the integrands that define $G_2(\tau)$ and $G_3(\tau)$ in powers of q and keeping the expansion up to $O(q^2)$, we obtain Eq. (6). This limit is valid provided that the reactions occur on a faster timescale than diffusion across the observation volume, i.e., if $\tau_{reac} \equiv [k_{off} + k_{on}(C_{eq} + F_{eq})]^{-1} \ll w_r^2/(4D_C)$ but is also good even if both timescales are of the same order of magnitude [18].

2. Limits of applicability of the fast reaction approximation

In order to study when the fast reaction approximation of the ACF can be used to estimate different biophysical parameters we computed numerically the full ACF, $G(\tau) = G_{\lambda_F} + G_{\lambda_1} + G_{\lambda_2}$, using the parameters of Table II and an adaptive Lobatto quadrature algorithm with the *quadl* function on MatLab [24] to compute Eqs. (A7) and (A8). We compared the results of these computations with the approximated ACF, $G_{approx}(\tau)$, given by Eqs. (6)–(9) using the same parameters. For the comparison we computed the difference between both functions given by

$$\varepsilon^2 = \frac{1}{n}\sum_{i=1}^{n}\left[G(\tau_i) - G_{approx}(\tau_i)\right]^2, \tag{A11}$$

with n the total number of data points. In Fig. 6(a) we plot ε^2 as a function of $[F4]_{tot}$ for high (solid line) and low (dashed line) affinity Fluo4. There we observe that, for both dyes, ε^2 first increases and then decreases with increasing $[F4]_{tot}$. The difference is larger for the low affinity dye attaining a maximum value, $\sim 3.3\,10^{-10}$, at $[F4]_{tot} \sim 3.7\,\mu$M. The maximum value, $\sim 1.1\,10^{-10}$ occurs at $[F4]_{tot} \sim 6.5\,\mu$M for the high affinity dye. $G(\tau)$ and $G_{approx}(\tau)$ are indistinguishable for the lowest dye concentrations used in the experiments, while $G_{approx}(\tau)$ decays faster with τ than $G(\tau)$ for the values, $[F4]_{tot}$, for which their difference is approximately maximal (data not shown).

We then analyzed what correlation times could be derived by fitting the full ACF with Eq. (5). The results of the fits depended on the time resolution with which we computed the ACF. Here we show the results of using the same resolution as in the experiments. For the fits, we probed two options. First, we fixed the timescales as in the fast reaction approximation and fitted the weights. Second, we fitted both the weights and the timescales. From the second test we determined that the fitted values obtained for τ_0, ν_F and the weights, g, g_1, and g_2, were similar to those prescribed by the fast reaction approximation. The other two fitted times differed slightly from those of the approximation. These results are illustrated in Fig. 6(b), where we show the ratios τ_0/τ_F, τ_1/τ_{ef1}, τ_2/τ_{ef2}, and ν_F/ν, between the fitted values and those of the fast reaction approximation for high affinity Fluo4. The difference, ε^2, between the fitted and the full ACF was less than $2.289\,10^{-10}$ using these fitting parameters. Similar results were obtained for low affinity Fluo4 with $\varepsilon^2 \leqslant 2.785\,10^{-10}$. Similar values of ε^2 ($2.278\,10^{-10}$ and $2.606\,10^{-10}$ for Fluo4 high and low affinity, respectively) were obtained when only the weights were fitted and the timescales were fixed at the fast reaction approximation values. We show in Fig. 6(c) the ratios between the fitted and the fast approximation weights for the high affinity Fluo4.

3. FCS experiments in aqueous solution and in *Xenopuslaevis* oocytes with tetramethylrhodamine-dextran to determine the factor by which free diffusion coefficients are rescaled in the cytoplasm

We here present the results of performing FCS experiments with tetramethylrhodamine-dextran (TMR-D) in aqueous solution and in *Xenopus laevis* oocytes. The aim of these experiments is to determine the conversion factor between free diffusion coefficients in the two media.

X. laevis oocytes, previously treated with collagenase and stored in Barth's solution, were loaded with 37 nl of TMR-D at different concentrations. Intracellular microinjections were performed using a Drummond microinjector. Assuming a 1 μl cytosolic volume, the final concentration of TMR-D was 0.9, 1.1, 1.4, or 1.85 μM. FCS measurements were performed on a spectral confocal scanning microscope FluoView 1000 (Olympus, Tokyo, Japan), employing a 60×, 1.35 N.A. oil-immersion objective (UPlanSAPO, Olympus) and a pinhole aperture of 115 μm. Single point measurements at a 50 kHz sampling rate were performed for a total duration of 167 s (equivalently, 8 365 312 data points) employing a 543-nm line and detecting the fluorescence in the range (555–655) nm. For the aqueous solutions the measurements were performed at $\sim$20 μm from the coverslip and for the oocytes, at the cortical granules region in the animal hemisphere. Experimental ACFs were calculated with a custom-made routine written on the Matlab platform [24]. To this end, each 167-s-long record was divided into $N_{sol} = 1021$, 164-ms-long segments containing 2^{13} points each for the experiments in aqueous solutions and into $N_{oo} = 510$, 328-ms-long segments containing 2^{14} points each for the experiments in *X. laevis* oocytes. The ACF was computed for each of the $N_{sol} = 1021$ or $N_{oo} = 510$ segments from which the average ACF was obtained. As the confocal volume dimensions are wavelength-dependent

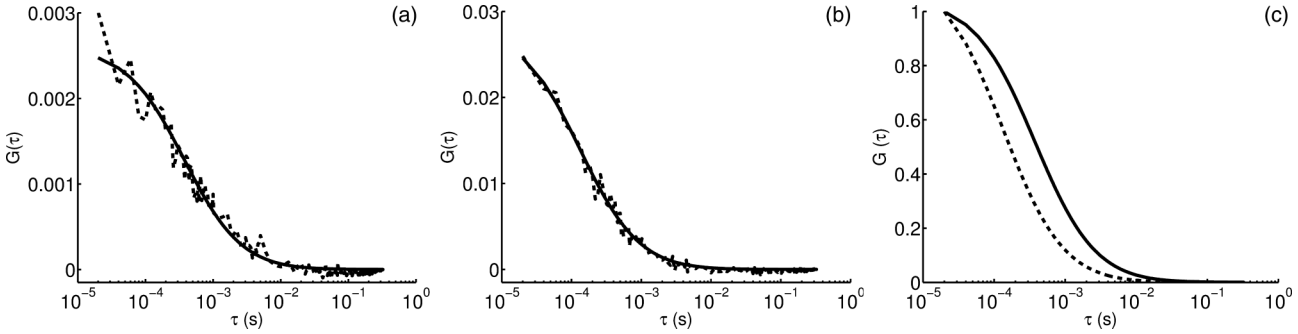

FIG. 7. (a) ACF obtained from FCS experiments performed in *X. laevis* oocytes microinjected with 37 nl of TMR-D = 30 μM (dashed line) fitted by Eq. (2) (solid line). (b) As in (a) for solution of TMR-D = 50 nM. (c) ACFs from the fits performed in (a) and (b) (solid and dashed line, respectively), normalized.

we used the FCS experiments with TMR-D in solution to estimate the beam waist and aspect ratio at 543 nm. Assuming a diffusion coefficient of $D_{\text{TMR-D}} = 85\ \mu\text{m}^2/s$ [26] we obtained $w_r = (0.199 \pm 0.003)\ \mu$m and $w = wz/wr = 5$. The ACF was fitted using only one (diffusive) component as in Eq. (2).

We show in Fig. 7 the ACF obtained from FCS experiments performed in *X. laevis* oocytes with TMR-D [Fig. 7(a)]. Using Eq. (2) to fit the data of Fig. 7, we obtain $D_{\text{TMR}}(\text{oocyte}) = (27 \pm 1)\ \mu\text{m}^2/\text{s}$. The TMR-D diffusion coefficient in solution is $D_{\text{TMR}}(\text{solution}) = 85\ \mu\text{m}^2/\text{s}$ [26]. Thus, it is $D_{\text{TMR-D}}(\text{oocyte})/D_{\text{TMR-D}}(\text{solution}) \sim 3$.

[1] B. Pando, S. P. Dawson, D.-O. D. Mak, and J. E. Pearson, Proc. Natl. Acad. Sci. USA **103**, 5338 (2006), retrieved from http://www.pnas.org/content/103/14/5338.full.pdf+html.

[2] S. L. Dargan and I. Parker, J. Physiol. **553**, 775 (2003).

[3] S. L. Dargan, B. Schwaller, and I. Parker, J. Physiol. **556**, 447 (2004).

[4] M. T. Nelson, H. Cheng, M. Rubart, L. F. Santana, A. D. Bonev, H. J. Knot, and W. J. Lederer, Science **270**, 633 (1995).

[5] N. Allbritton, T. Meyer, and L. Stryer, Science **258**, 1812 (1992).

[6] R. M. Paredes, J. C. Etzler, L. T. Watts, W. Zheng, and J. D. Lechleiter, Methods **46**, 143 (2008).

[7] E. Piegari, L. Lopez, E. P. Ipiña, and S. P. Dawson, PLoS ONE **9**, 0095860 (2014).

[8] A. C. Ventura, L. Bruno, A. Demuro, I. Parker, and S. P. Dawson, Biophys. J. **88**, 2403 (2005).

[9] L. Bruno, G. Solovey, A. C. Ventura, S. Dargan, and S. P. Dawson, Cell Calcium **47**, 273 (2010).

[10] E. Elson, Biophys. J. **101**, 2855 (2011).

[11] D. Magde, E. Elson, and W. W. Webb, Phys. Rev. Lett. **29**, 705 (1972).

[12] E. L. Elson, Traffic **2**, 789 (2001).

[13] E. Haustein and P. Schwille, Annu. Rev. Biophys. Biomol. Struct. **36**, 151 (2007), retrieved from http://www.annualreviews.org/doi/pdf/10.1146/annurev.biophys.36.040306.132612.

[14] G. Kaur, M. W. Costa, C. M. Nefzger, J. Silva, J. C. Fierro-Gonzalez, J. M. Polo, D. M. Bell, and N. Plachta, Nat. Commun. **4**, 1637 (2013).

[15] N. L. Thompson, in *Topics in Fluorescence Spectroscopy: Techniques*, edited by J. R. Lakowicz (Springer US, Boston, MA, 1999), pp. 337–378.

[16] D. C. Lamb, A. Schenk, C. Röcker, C. Scalfi-Happ, and G. U. Nienhaus, Biophys. J. **79**, 1129 (2000).

[17] E. Bismuto, E. Gratton, and D. C. Lamb, Biophys. J. **81**, 3510 (2001).

[18] E. P. Ipiña and S. P. Dawson, Phys. Rev. E **87**, 022706 (2013).

[19] E. P. Ipiña and S. P. Dawson, Biophys. J. **107**, 2674 (2014).

[20] L. Sigaut, M. L. Ponce, A. Colman-Lerner, and S. P. Dawson, Phys. Rev. E **82**, 051912 (2010).

[21] L. Sigaut, J. E. Pearson, A. Colman-Lerner, and S. P. Dawson, PLoS Comput. Biol. **10**, e1003629 (2014).

[22] A. A. Arish, A. Porcher, A. Czerwonka, N. Dostatni, and C. Fradin, Biophys. J. **99**, L33 (2010).

[23] T. Gregor, D. W. Tank, E. F. Wieschaus, and W. Bialek, Cell **130**, 153 (2007).

[24] MATLAB, *version 7.10.0 (R2010a)* (MathWorks Inc., Natick, MA, 2010).

[25] C. T. Culbertson, S. C. Jacobson, and J. M. Ramsey, Talanta **56**, 365 (2002).

[26] A. Gennerich and D. Schild, Biophys. J. **83**, 510 (2002).

[27] D. Qin, A. Yoshida, and A. Noma, Japan. J. Physiol. **41**, 333 (1991).

[28] W. M. Haynes, *CRC Handbook of Chemistry and Physics 2015-2016* (CRC Press, Boca Raton, FL, 2015).

[29] F. v. Wegner, N. Wieder, and R. H. Fink, Front. Genet. **5** (2014).

[30] M. Wachsmuth, C. Conrad, J. Bulkescher, B. Koch, R. Mahen, M. Isokane, R. Pepperkok, and J. Ellenberg, Nat. Biotechnol. **33**, 384 (2015).

[31] A. Biess, E. Korkotian, and D. Holcman, PLoS Comput. Biol. **7**, 1002182 (2011).

[32] P. C. Bressloff and J. M. Newby, Rev. Mod. Phys. **85**, 135 (2013).

[33] E. Piegari, L. Sigaut, and S. P. Dawson, Cell Calcium **57**, 109 (2015).

[34] A. Diaspro, F. Federici, and M. Robello, Appl. Opt. **41**, 685 (2002).

[35] J. Enderlein, I. Gregor, D. Patra, and J. Fitter, Curr. Pharm. Biotechnol. **5**, 155 (2004).

[36] J. Enderlein, I. Gregor, D. Patra, T. Dertinger, and U. B. Kaupp, Chem. Phys. Chem. **6**, 2324 (2005).
[37] C.-Y. Tan and Y.-X. Huang, J. Chem. Eng. Data **60**, 2827 (2015).
[38] R. Tsien, in *Calcium as a Cellular Regulator*, edited by E. Carafoli and C. Klee (Oxford University Press, New York, 1999), pp. 28–54.
[39] M. Naraghi, Cell Calcium **22**, 255 (1997).
[40] L. Wawrezinieck, H. Rigneault, D. Marguet, and P.-F. Lenne, Biophys. J. **89**, 4029 (2005).
[41] P.-F. Lenne, L. Wawrezinieck, F. Conchonaud, O. Wurtz, A. Boned, X.-J. Guo, H. Rigneault, H.-T. He, and D. Marguet, EMBO J. **25**, 3245 (2006).
[42] C. D. Rienzo, V. Piazza, E. Gratton, F. Beltram, and F. Cardarelli, Nat. Commun. **5**, 5891 (2014).
[43] M. D. White, J. F. Angiolini, Y. D. Alvarez, G. Kaur, Z. W. Zhao, E. Mocskos, L. Bruno, S. Bissiere, V. Levi, and N. Plachta, Cell **165**, 75 (2016).
[44] O. Krichevsky and G. Bonnet, Rep. Prog. Phys. **65**, 251 (2002).